A Method for Modeling Adjustable Throat-Area Expansion Valves Using Manufacturers' Rating Data

Haorong Li, PhD
Member ASHRAE

James E. Braun, PhD, PE
Fellow ASHRAE

Received July 27, 2007; accepted March 26, 2008

Adjustable throat-area expansion valves (ATAEVs), including thermostatic and electric expansion valves, are used commonly in air-conditioning equipment and lead to improved system performance as compared to the use of fixed-orifice expansion devices. However, ATAEV modeling literature is limited. Typically, an ATAEV is modeled by specifying the superheat entering the compressor or by empirically correlating experimental data. In order to model system behavior more accurately and effectively over a wide range of conditions, more accurate ATAEV models are necessary and a more general modeling methodology is desired. This paper presents a general model format that utilizes manufacturers' rating data. Model structures for three types of valve geometries are derived. Two model formats and corresponding parameter estimation procedures using manufacturer performance rating data are considered. The proposed method is validated using experimental data and compared with results from the literature. Both the experimental validation and the theoretical analysis demonstrate that the proposed method is more accurate and more generic than other methods presented in the literature.

INTRODUCTION

Expansion devices reduce the pressure and regulate the refrigerant flow to the low-side evaporator within a vapor-compression system. A model of the expansion device is essential for simulating the whole system and can be used as a virtual sensor to estimate its upstream pressure as part of an automated diagnostic system (Li and Braun 2004).

There are two kinds of expansion devices used in vapor-compression systems: fixed-area and adjustable throat-area devices. The drawback associated with fixed-area devices is their limited ability to efficiently regulate refrigerant flow in response to changes in system operating conditions, as they are sized based on one set of conditions. Adjustable throat-area expansion valves (ATAEVs) provide a better solution to regulating refrigerant flow into a direct expansion type evaporator using feedback control. A thermostatic expansion valve (TXV) and an electric expansion valve (EXV) are two types of ATAEVs. A TXV is a completely mechanical device that uses a single variable proportional feedback control scheme to maintain a nearly constant superheat at the evaporator outlet. The fundamental principle of an EXV is the same as that of a TXV except that it uses electronic actuation and sensor information along with a digital feedback controller and can theoretically operate with a smaller degree of superheat than a TXV. There is a lot of literature for modeling and experimental investigations of fixed-orifice devices, but although TXVs and EXVs are used more and more widely, there is very little literature related to modeling their behaviors. In some simulation models for unitary heat pumps, such as PUREZ (Rice and Jackson

Haorong Li is an assistant professor of Architectural Engineering at the University of Nebraska-Lincoln, Omaha, NE. **James E. Braun** is a professor of Mechanical Engineering at Purdue University, West Lafayette, IN.

1994), models for TXVs and EXVs are simplified by explicitly fixing a constant superheat or implicitly specifying superheat trends. Browne and Bansal (1998) describe a modeling method using the difference between the superheat in the evaporator and the reference superheat temperature to modify the fixed-orifice model. Harms (2002) showed that constant superheat was a poor assumption and correlated TXV performance using experimental data. Among the limited literature, none discuss fundamentally whether the flow is choked or not. In the limited literature, the following format for an ATAEV model has been generally adopted:

$$\dot{m} = C_d A \sqrt{\rho(P_{up} - P_{down})} \tag{1}$$

where C_d is the discharge coefficient, A is the throat area, ρ is density, P_{up} is the upstream pressure, and P_{down} is the downstream pressure. The above equation is the same as that for an orifice except that A is a variable. With this model, mass flow rate is a strong function of pressure drop $\Delta P = P_{up} - P_{down}$ and variable restriction area A but a very weak function of upstream refrigerant subcooling, T_{sub}.

This paper employs the model form of Equation 1. It is important to note that this approach contains the implicit assumption that the flow is not choked. This may not always be the case. In early work on this topic, Benjamin and Miller (1941) conducted experiments of sharp-edged orifices of $L/D = 0.28 \sim 1$ with saturated water at various upstream pressures and found that orifices having $L/D < 1$ did not choke the flow at normal operating conditions. On the other hand, some researchers (Chisholm 1967; Krakow and Lin 1988) observed that the mass flow rate of a refrigerant through an orifice in a heat pump was primarily dependent on the upstream conditions rather than on the pressure drop across the valve, which indicates that the flow could be choked. Recent findings by some researchers (Kim et al. 2002; Bullard 2007) observed that the exit plane pressure was likely closer to the flashing pressure, which indicates that even if the flow is choked the above model format can be used. Although this paper includes validation of the format of Equation 1 for a few cases, it is advisable to evaluate its applicability for each application where the model might be employed. This is possible using manufacturers' data and following the procedures illustrated in this paper.

APPROACH

In this section, the general model format is validated using manufacturers' data, mathematical expressions are derived that relate throttle area to valve position and valve position to superheat, and procedures are presented for estimating model parameters from manufacturers' rating data.

Model Format Validation Using Manufacturers' Rating Data

The validity of the model format in Equation 1 can be checked indirectly by analyzing manufacturers' rating data. Equation 1 can be rearranged as

$$C_d A = \frac{\dot{m}_{ref}}{\sqrt{\rho(P_{up} - P_{down})}} . \tag{2}$$

According to *ANSI/ASHRAE Standard 17, Method of Testing Capacity of Thermostatic Refrigerant Expansion Valves* (ASHRAE 1998a) and *ARI Standard 750, Thermostatic Refrigerant Expansion Valves* (ARI 2001), throat area A is nearly fixed by fixing the opening superheat when generating the manufacturers' rating data for a TXV. For an EXV, the throat area A is exactly fixed at the rating value. So $C_d A_{rated}$ for a TXV should be relatively constant if the flow is not choked and that for an EXV should be constant.

Figure 1 shows that C_dA_{rated} for a 3.5-ton EXV is pretty constant (mean: 2.574 mm^2, standard variation: 0.004 mm^2) over the whole set of rating conditions (evaporator temperature: –40°C ~ 5°C, pressure drop: 3 ~ 17 bar).

Figure 2 shows that for a 5-ton TXV, C_dA_{rated} has an abrupt change from an air-conditioning application (evaporator temperature: –5°C ~ 5°C) to a refrigeration application (evaporator temperature: –15°C). In spite of the abrupt change, its overall variation is still small (mean: 3.484 mm^2, standard variation: 0.102 mm^2). However, the variation is very small within each application range. For air-conditioning applications, the mean is 3.554 mm^2 and standard variation is 0.007 mm^2. For refrigeration applications, the mean is 3.345 mm^2 and standard variation is 0.004 mm^2. Similar results can be obtained through checking more manufacturers' rating data. Therefore, the ATAEV model format in Equation 2 is accurate at the rating conditions and the flow does not appear to be choked.

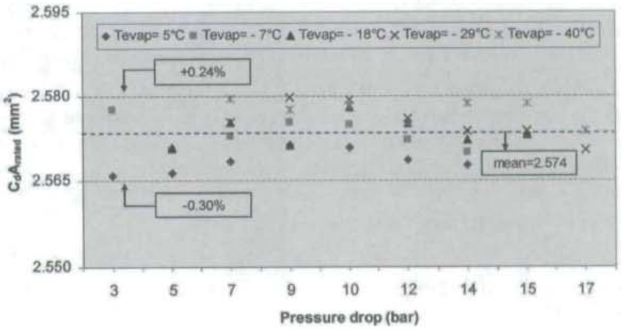

Figure 1. C_dA_{rated} values for an EXV at manufacturers' rating conditions.

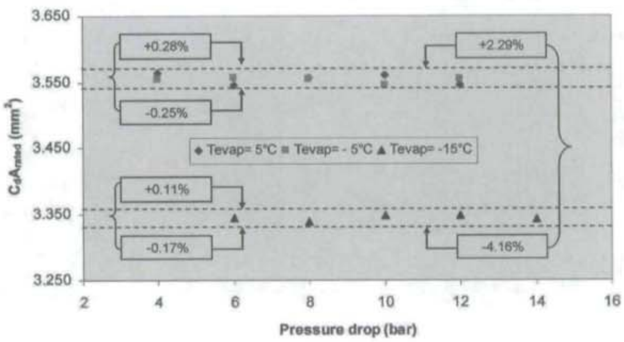

Figure 2. C_dA_{rated} values for a TXV at manufacturers' rating conditions.

The abrupt change in $C_d A_{rated}$ for the TXV can be explained by the saturation pressure-temperature (P-T) curve for the thermostatic charge fluid. Figure 3 shows that the P-T curve becomes flatter at lower temperatures. As a result, a given opening superheat results in less pressure difference across the valve diaphragm at lower evaporating temperatures, causing a reduction in valve opening area. For example, the pressure difference caused by 5°C of opening superheat at an evaporating temperature of 5°C is 0.969 bars, which is far larger than 0.584 bars at an evaporating temperature of −15 °C. Fortunately, this would not cause any problem in modeling because 1) the P-T curve is pretty linear if it is divided into three sections—AB, BC, and CD; 2) for a given application, the TXV will work in one of the three sections and the TXV used in packaged air conditioning falls into section CD; and 3) the nonlinearity can be eliminated or overcome using liquid cross charges. For liquid-cross-charged TXVs operating within their intended range of evaporating temperatures, the TXV working fluid is chosen so that the opening force is nearly proportional to the opening superheat (ASHRAE 1998b).

In summary, from manufacturers' standard rating data, the flow across a TXV or EXV is either not choked or, as observed by Kim et al. (2002) and Bullard (2007), the exit plane pressure was closer to the flashing pressure. In either case, the model format of Equation 1 is valid. To specify a TXV or EXV model, the key point is to find an expression for variable throat area, A, in terms of superheat and then specify the constant C_d using manufacturers' rating data.

Generally speaking, the throat area, A, is a function of valve position, which is determined by the control strategy used by the valve. Because TXVs and EXVs use different control strategies, the first step is to derive A in terms of valve position and then develop expressions for valve position in terms of superheat.

Derivation of Throat-Area Expression

As shown in Figure 4, there are three kinds of valves used in TXVs and EXVs. Among them, types I and II are used widely and their geometric model is the same.

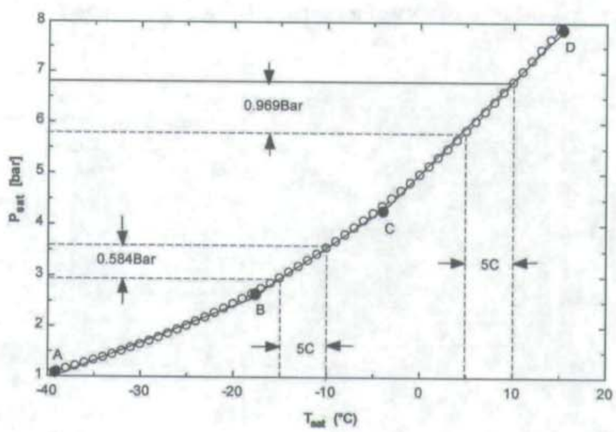

Figure 3. Pressure-temperature saturation curve for R-22.

Figure 5a illustrates a TXV valve at an operating point for a type I or II valve. For this geometry, the throat area at a certain valve position, h, is

$$A = \frac{\pi}{4}(D^2 - d^2) \ , \tag{3}$$

where $d = 2\tan\theta(H - h)$ and $\tan\theta = \dfrac{D}{2H}$, so

$$d = 2\frac{D}{2H}(H-h) = D\left(1 - \frac{h}{H}\right) \ . \tag{4}$$

These equations can be combined to give

$$A = \frac{\pi}{4}\left(D^2 - D^2\left(1 - \frac{2h}{H} + \left(\frac{h}{H}\right)^2\right)\right) = \frac{\pi}{2}D^2\left(\frac{h}{H} - \frac{1}{2}\left(\frac{h}{H}\right)^2\right) = \frac{\pi}{4}\frac{h}{H}D^2\left(2 - \frac{h}{H}\right) \tag{5}$$

The throat area, A, is a second-order function of valve position h, which is plotted in Figure 5c.

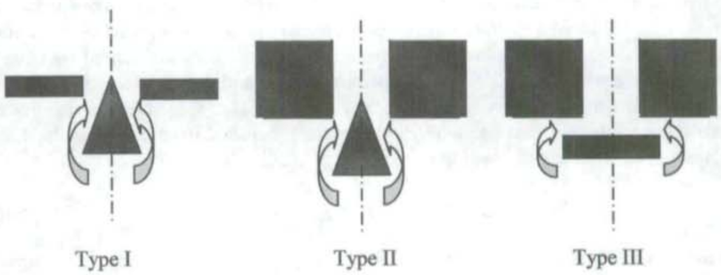

Figure 4. Three types of valve geometry.

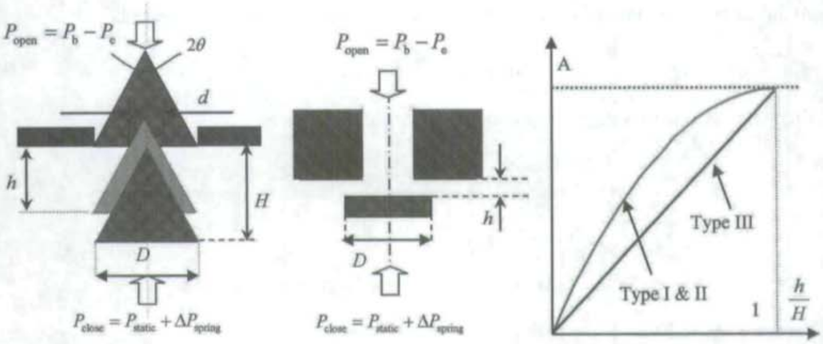

(a) Geometric model of types I & II valves (b) Geometric model of a type III valve (c) Relationship between valve position and throat area

Figure 5. Geometric models and throat-area curves for different valve types.

Figure 5b depicts the geometric model for valve type III. An expression for throat area in terms of valve position is

$$A = \pi D h \ . \tag{6}$$

It can be seen that the throat area, A, is a linear function of the valve position, h. It is plotted in Figure 5c.

Valve Position Expression

The valve position for an EXV can be calculated easily from the control signal,

$$h = f(u_{ctrl}) \ , \tag{7}$$

where u_{ctrl} is determined by the control algorithm and can be a function of various thermodynamic parameters.

For a TXV, valve position is a function of superheat. As illustrated in Figures 5a and 5b, the pressure of the thermostatic element, P_b, is applied to the top of a diaphragm and acts to open the valve; the evaporator temperature, P_e, is applied under the diaphragm and acts in a closing direction; P_{static} is caused by the initial spring deformation, which is preset by an initial static superheat setting and acts to close the valve; ΔP_{spring} is the pressure caused by extra spring deformation other than the initial static superheat setting and acts to close the valve. So, the time-varying pressure difference between P_b and P_e acts to open the valve. Assume that the P-T curve is linear in the range of operation, and then the pressure difference across the diaphragm (P_{open}) is a linear function of opening superheat, $T_{sh,opening}$,

$$P_{open} = P_b - P_e = k_1 T_{sh,operating} \ , \tag{8}$$

and according to Hooke's Law, the total spring force, P_{close}, is proportional to the total spring deformation,

$$P_{close} = P_{static} + \Delta P_{spring} = k_2(x_{static} + h) \ . \tag{9}$$

At any constant operating condition, the forces exerted on the valve are balanced:

$$k_1 T_{sh,\,operating} = k_2(x_{static} + h) \tag{10}$$

Rearranging Equation 10 gives an expression for valve position:

$$\begin{aligned} h &= \frac{k_1}{k_2} T_{sh,\,operating} - x_{static} = kT_{sh,\,operating} - x_{static} = kT_{sh,\,operating} - kT_{sh,\,static} \\ &= k(T_{sh,\,operating} - T_{sh,\,static}) = kT_{sh,\,opening} \end{aligned} \tag{11}$$

As shown in Figure 6a, the valve position is a linear function of opening superheat.

Overall Mass Flow Rate Model for a TXV

For an EXV, an overall mass flow rate model can be obtained by substituting the throat area into Equation 1 and coupling the valve position to a specific feedback controller algorithm. An overall mass flow rate model for a TXV can be obtained by substituting the expressions for throat area and valve position into the general model equation.

For type I and II valves, this leads to:

$$
\begin{aligned}
A &= \frac{\pi D^2}{4}\frac{h}{H}\left(2-\frac{h}{H}\right) = \frac{\pi D^2}{4}\frac{kT_{sh,\,opening}}{H}\left(2-\frac{kT_{sh,\,opening}}{H}\right) \\
&\frac{\pi D^2}{4}\frac{kT_{sh,\,opening}}{kT_{sh,\,max,\,opening}}\left(2-\frac{kT_{sh,\,opening}}{kT_{sh,\,max,\,opening}}\right) = \frac{\pi D^2}{4}\frac{T_{sh,\,opening}}{T_{sh,\,max,\,opening}}\left(2-\frac{T_{sh,\,opening}}{T_{sh,\,max,\,opening}}\right)
\end{aligned} \tag{12}
$$

$$
\begin{aligned}
\dot{m} &= C_d A\sqrt{\rho(P_{up}-P_{down})} = C_d\frac{\pi D^2}{4}\frac{T_{sh,\,opening}}{T_{sh,\,max,\,opening}}\left(2-\frac{T_{sh,\,opening}}{T_{sh,\,max,\,opening}}\right)\sqrt{\rho(P_{up}-P_{down})} \\
&= C_{\text{I-II}}\left(2\frac{T_{sh,\,opening}}{T_{sh,\,max,\,opening}}-\left(\frac{T_{sh,\,opening}}{T_{sh,\,max,\,opening}}\right)^2\right)\sqrt{\rho(P_{up}-P_{down})}
\end{aligned} \tag{13}
$$

where $C_{\text{I-II}}$ (= $C_d\frac{\pi D^2}{4}$) is a constant for type I and II valves.

For type III valves:

$$A = \pi D k T_{sh,\,opening} \tag{14}$$

$$
\begin{aligned}
\dot{m} &= C_d A\sqrt{\rho(P_{up}-P_{down})} = C_d\pi D k T_{sh,\,opening}\sqrt{\rho(P_{up}-P_{down})} \\
&= C_{\text{III}} T_{sh,\,opening}\sqrt{\rho(P_{up}-P_{down})}
\end{aligned} \tag{15}
$$

where C_{III} (= $C_d\pi Dk$) is a constant for type III valve.

Figure 6b shows refrigerant mass flow rate versus superheat for a fixed pressure drop. It can be seen that:

1. The mass flow rate for type I and II valves is higher than that for type III valves with the same operating range and at the same superheat, except when the valves are fully open or

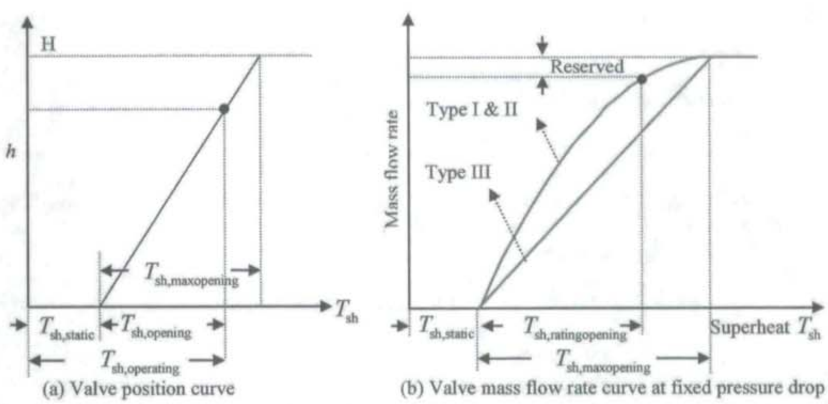

Figure 6. Valve position and mass flow rate curves.

closed. Therefore, for valves with the same operating range, type I and II valves require smaller superheat to get the same capacity as type III valves.

2. The mass flow for type III valves increases linearly with superheat until the maximum opening superheat is reached, whereas the mass flow rate for type I and II valves increases nonlinearly and the rate of increase approaches zero when the valve is fully open. When the valve is fully open, the mass flow is larger than that at the rating condition and so is the capacity. The additional capacity beyond the rating condition is termed *reserve capacity*. Since the rate of increase in mass flow rate decreases with opening, type III valves require more superheat than type I and II valves to achieve the same reserve capacity. In other words, type I and II valves would be expected to have smaller reserve capacity (around 10%) than type III valves (up to 40%) in order to avoid abnormally high superheat at a high-capacity operation. However, an advantage of type I and II valves is a reduction in TXV cycling ("hunting") caused by the TXV alternately overfeeding and underfeeding the evaporator.

Model Parameter Estimation Methods

Since the overall mass flow rate model for EXVs is explicit, all the parameters are available. For TXVs, from the above analysis it can be seen that the mass flow rate for type I and II TXVs is a nonlinear function of superheat while that of type III is a linear function of superheat. However, in most of the existing literature, it is assumed that the mass flow rate for any TXV is a linear function of superheat. So, in order to simplify the parameter estimation, a globally linear assumption can be adopted (no approximation for type III TXV). Alternatively, the nonlinear model can be employed with a more complicated method for estimating parameters with additional assumptions. Both approaches are considered in this section.

Globally Linear Model. Under the globally linear assumption, the general TXV model is

$$\dot{m} = C_{linear}(T_{sh,\,operating} - T_{sh,\,static})\sqrt{\rho(P_{up} - P_{down})} \ , \tag{16}$$

where C_{linear} is a constant. Rearranging Equation 16 gives

$$C_{linear}(T_{sh,\,operating} - T_{sh,\,static}) = \frac{\dot{m}}{\sqrt{\rho(P_{up} - P_{down})}} \ . \tag{17}$$

The parameters of this TXV model can be determined using the following procedure:

1. According to manufacturers' rating data,

$$C_{linear}(T_{sh,\,rating} - T_{sh,\,static}) = C_{linear}T_{sh,\,rating,\,opening} = \text{CONSTANT} \ , \tag{18}$$

where $T_{sh,rating,opening}$ is fixed by the TXV manufacturer and should be readily available. Although the TXV manufacturer presets the $T_{sh,static}$ as well, the manufacturer of an air-conditioning system would adjust it slightly in order to match the rated capacity.

2. If $T_{sh,rating,opening}$ is available from the manufacturer, go to step 3. If not, estimate an initial value according to ARI (2001) and ASHRAE (1998a) standards and manufacturing tradition (see Table 1).
3. Determine $C_{linear} = \dfrac{\text{CONSTANT}}{T_{sh,\,rating,\,opening}}$.
4. Determine $T_{sh,static}$. If the number of rotations adjusted by the system manufacturer is recorded, it could be easy to calculate the actual static superheat. If not, it could be estimated from the manufacturer settings and refined by experimental data.

Table 1. TXV Rating Settings

Source	$T_{sh,rating,opening}$, °C	$T_{sh,rating}$, °C	$T_{sh,static}$, °C	Reserve Capacity
ARI Standard 750 (ARI 2001)	≤4		>1	
ASHRAE Standard 17 (ASHRAE 1998a)	3		3	
ASHRAE Handbook (ASHRAE 1998b)	2 ~ 4			0.1 ~ 0.4
Manufacturer A (recommend)	2.2 ~ 3.3		3.3 ~ 5.6	
Manufacturer B (recommend)		4.4 ~ 6.7		
Recommended Initial Guess	3 or 4		3, 4 or 5	0.1

5. Determine $T_{sh,max,opening}$ using the manufacturers' tradition of reserving capacity, $Cap_{reserve}$, to set the upper boundary of $(T_{sh,rating} - T_{sh,static})$.

$$\frac{T_{sh,\,rating,\,opening}}{T_{sh,\,max,\,opening}} \approx 1 - Cap_{reserve} \tag{19}$$

Nonlinear Model. The nonlinear model format is

$$\dot{m} = C_{nonlinear}\left(2\frac{T_{sh,\,opening}}{T_{sh,\,max,\,opening}} - \left(\frac{T_{sh,\,opening}}{T_{sh,\,max,\,opening}}\right)^2\right)\sqrt{\rho(P_{up} - P_{down})}, \tag{20}$$

where $C_{nonlinear}$ is a constant. Rearranging Equation 20 gives:

$$C_{nonlinear}\left(2\frac{T_{sh,\,opening}}{T_{sh,\,max,\,opening}} - \left(\frac{T_{sh,\,opening}}{T_{sh,\,max,\,opening}}\right)^2\right) = \frac{\dot{m}}{\sqrt{\rho(P_{up} - P_{down})}} \tag{21}$$

The parameters of the nonlinear TXV model can be determined using the following procedure:

1. According to manufacturers' rating data,

$$C_{nonlinear}\left(2\frac{T_{sh,\,rating,\,opening}}{T_{sh,\,max,\,opening}} - \left(\frac{T_{sh,\,rating,\,opening}}{T_{sh,\,max,\,opening}}\right)^2\right) = \text{CONSTANT}\ . \tag{22}$$

2. According to manufacturers' tradition of reserving capacity,

$$\left(2\frac{T_{sh,\,rating,\,opening}}{T_{sh,\,max,\,opening}} - \left(\frac{T_{sh,\,rating,\,opening}}{T_{sh,\,max,\,opening}}\right)^2\right) \approx 1 - Cap_{reserve} \tag{23}$$

$$\Rightarrow C_{nonlinear} = \frac{\text{CONSTANT}}{1 - Cap_{reserve}} \tag{24}$$

and solving the equation,

$$\frac{T_{sh,\,rating,\,opening}}{T_{sh,\,max,\,opening}} = 1 - \sqrt{Cap_{reserve}}\ . \tag{25}$$

3. Determine $T_{sh,static}$ and $T_{sh,rating,opening}$ as described in the global linear model section.
4. Determine $T_{sh,max,opening}$ and set the upper boundary for $(T_{sh,rating} - T_{sh,static})$.

CASE STUDY

Data for a 5-ton rooftop air conditioner collected by Harms (2002) were used to validate the TXV model. The rooftop air conditioner used R-22 as a refrigerant and a type I TXV as an expansion device. As shown in Table 2, the testing was conducted under four sets of operating conditions. For each set of conditions, seven test points were collected (except that there was only one valid test point for the HT test condition). Each point represents a specific refrigerant charge level. Due to significant variations in charge levels, the valve inlet subcooling varied from 0.62°C to 14.40°C.

Globally Linear Model

According to the manufacturers' rating data,

$$C_{linear}(T_{sh,\,rating} - T_{sh,\,static}) = \text{CONSTANT} = 3.5576\ \text{mm}^2\ . \tag{26}$$

From experimental data set A from Harms (2002) with a nominal charge, it can be estimated that

$$T_{sh,\,rating} = 8°\text{C}\ . \tag{27}$$

Assuming $T_{sh,\,rating,\,opening} = 4°\text{C}$,

$$T_{sh,\,static} = T_{sh,\,rating} - T_{sh,\,rating,\,opening} = 8 - 4 = 4°\text{C} \tag{28}$$

and

$$C_{linear} = \frac{3.5576}{4} = 0.8894\ . \tag{29}$$

Assuming the reserve capacity is 10%, since most valves are type I and II,

$$T_{sh,\,max,\,opening} \approx \frac{T_{sh,\,rating,\,opening}}{1 - Cap_{reserve}} = \frac{4}{0.9} \approx 4.5°\text{C}\ . \tag{30}$$

So,

$$\begin{aligned}\dot{m} &= C_{linear}(T_{sh,\,operating} - T_{sh,\,static})\sqrt{\rho(P_{up} - P_{down})} \\ &= 0.8894(T_{sh,\,operating} - 4)\sqrt{\rho(P_{up} - P_{down})}\end{aligned}\ , \tag{31}$$

where the upper boundary of $(T_{sh,rating} - T_{sh,static})$ is set at 4.5°C and the unit for P_{up} and P_{down} is Pa.

Table 2. Testing Conditions

Test Conditions	Air Entering Outdoor Coil: Dry-Bulb, °C	Air Entering Indoor Coil: Dry-Bulb, °C	Air Entering Indoor Coil: Wet-Bulb, °C	Refrigerant Charge Level: % Nominal Charge	Number of Points	Valve Inlet Subcooling Range, °C
A	35.00	26.67	19.47	86 ~ 144	7	1.72~14.01
B	27.78	26.67	19.47	78 ~ 127	7	0.62~ 9.90
C	27.78	26.67	< 13.93	80 ~ 148	7	1.60~ 14.40
HT	48.89	26.67	19.47	86	1	1.31

Nonlinear Model

According to the manufacturers' rating data,

$$C_{nonlinear}\left(2\frac{T_{sh,\,rating,\,opening}}{T_{sh,\,max,\,opening}} - \left(\frac{T_{sh,\,rating,\,opening}}{T_{sh,\,max,\,opening}}\right)^2\right) = \text{CONSTANT} = 3.5576\ \text{mm}^2\ . \tag{32}$$

Assuming reserve capacity of 10%,

$$C_{nonlinear} = \frac{\text{CONSTANT}}{1 - Cap_{reserve}} = \frac{3.5576}{0.9} = 3.9529 \tag{33}$$

and

$$\frac{T_{sh,\,rating,\,opening}}{T_{sh,\,max,\,opening}} = 1 - \sqrt{Cap_{reserve}} = 1 - \sqrt{0.1} = 0.68\ . \tag{34}$$

Assuming $T_{sh,\,rating,\,opening} = 4°\text{C}$,

$$T_{sh,\,maxopening} = \frac{4}{0.68} \approx 6°\text{C}\ , \tag{35}$$

so

$$\begin{aligned} \dot{n} &= C_{nonlinear}\left(2\frac{T_{sh,\,opening}}{T_{sh,\,max,\,opening}} - \left(\frac{T_{sh,\,opening}}{T_{sh,\,max,\,opening}}\right)^2\right)\sqrt{\rho(P_{up} - P_{down})} \\ &= 3.9529\left(2\frac{T_{sh,\,opening}}{6} - \left(\frac{T_{sh,\,opening}}{6}\right)^2\right)\sqrt{\rho(P_{up} - P_{down})} \end{aligned}\ , \tag{36}$$

where the upper boundary of $(T_{sh,rating} - T_{sh,static}) = T_{sh,opening}$ is set at 6°C and the unit for P_{up} and P_{down} is Pa.

Results Comparison

Harms (2002) plotted all four sets of data (see Figure 7) and fit the following model by minimizing the least squares error.

$$\dot{m}_{ref} = c_1(T_{sh,\,operating} - c_2)[\rho(P_{up} - P_{down})]^{0.5} \tag{37}$$

Harms determined $c_1 = 0.51\ \text{mm}^2/°\text{C}$, $c_2 = 1.0°\text{C}$. So,

$$\dot{m} = 0.51(T_{sh,\,operating} - 1)\sqrt{\rho(P_{up} - P_{down})}\ , \tag{38}$$

where the upper boundary of $T_{sh,operating} - 1$ was set at 8°C.

Figure 8 and Table 3 show results for the globally linear and nonlinear modeling approaches along with results from a correlation model presented by Harms (2002). The model developed by Harms used all of the experimental data in Figure 8 to train the model. It is obvious that the nonlinear model provides better predictions than the globally linear model and shows comparable accuracy to the interpolation performance of Harms's regression model.

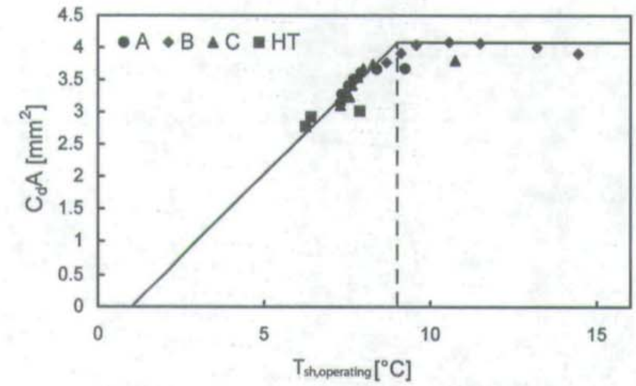

Figure 7. C_dA values for a 5-ton RTU TXV as a function of superheat.

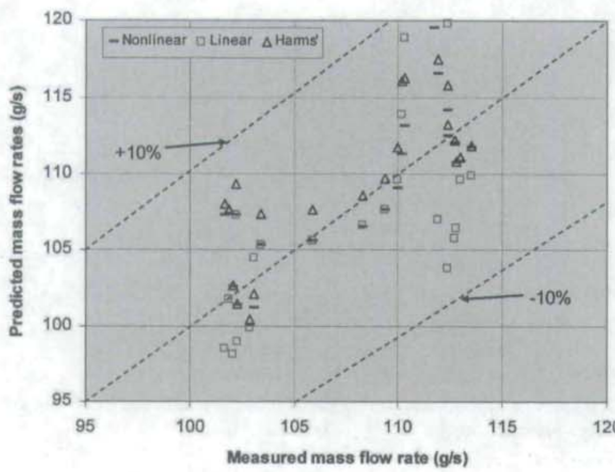

Figure 8. Comparison of three models' predictions.

Table 3. Comparison of Relative Errors for Mass Flow Rate Predictions

Relative Errors	Nonlinear Model	Global Linear Model	Harms's Regression Model
Mean	0.0096	−0.0043	0.0235
Standard deviation	0.0291	0.0460	0.0352
Maximum	0.06985	0.08822	0.1092
Minimum	−0.02686	−0.07647	−0.0237
Spread	0.0967	0.1647	0.1329

Although Harms's empirical model may be good for interpolation, it can not be expected to extrapolate well. Mathematically, this model is equivalent to making a locally linear assumption (see Figure 9). If the experimental data range is limited, parameters c_1 and c_2 will be unreasonable. For example, Harms's 5-ton rooftop unit's parameter c_2, which is supposed to be the static superheat setting, is equal to 1°C, while the upper boundary of opening superheat is set at 8°C. According to ARI (2001) and ASHRAE (1998a) standards, static superheat should be far larger than 1°C, and 8°C for an upper boundary on opening superheat (indicating 50% of reserve capacity) is too large. For a 7.5-ton rooftop unit considered by Harms, parameter c_2 was correlated to be a negative value, –4.4°C, which is physically impossible.

CONCLUSIONS

The general model format used for adjustable-area expansion devices in the literature was validated using manufacturers' data, which demonstrates that the flow through adjustable-area expansion devices is probably not choked. Expressions for throat areas were derived as a function of valve position and superheat, which leads to a mass flow rate model. Two model formats and corresponding parameter estimation procedures using manufacturer performance rating data were proposed. The model prediction performance was compared with laboratory measurements and results in the literature. Both the nonlinear and globally linear models can have much better extrapolation performance than empirical regression models, such as that proposed by Harms (2002). The nonlinear model provides better predictions over a wide range of operating conditions than the globally linear model and comparable accuracy to the interpolation performance of the empirical regression model of Harms (2002).

It is important to note that the modeling approach based on Equation 1 contains the implicit assumption that the flow is not choked. Although this paper includes validation of the format of Equation 1 for a few cases, it is advisable to evaluate its applicability for each application where

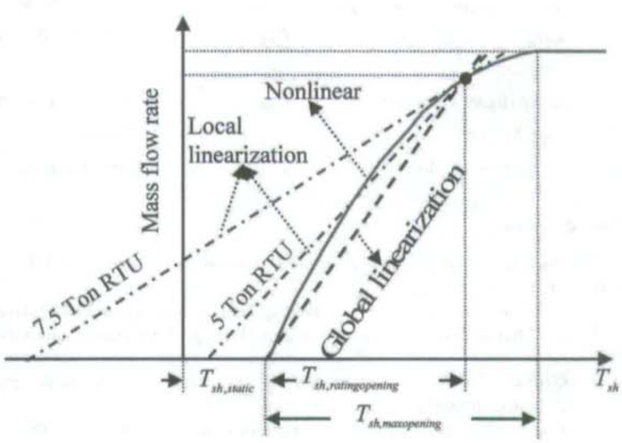

Figure 9. Illustration of the three modeling methods.

the model might be employed. This is possible using manufacturers' data and following the procedures illustrated in this paper.

NOMENCLATURE

A = throat area
C_d = discharge coefficient
C_dA = product of discharge coefficient and throat area
C_dA_{rated} = C_dA at rated conditions
C_{linear} = constant for a linear valve model
$C_{nonlinear}$ = constant for a nonlinear valve model
$C_{I\text{-}II}$ = constant for type I and II valves
C_{III} = constant for type III valve
d = acting valve disc diameter
D = maximum valve disc diameter
ΔP = pressure drop
ΔP_{spring} = pressure caused by spring deformation
h = acting valve disc position
H = maximum valve disc position
k = ratio of k_1 to k_2
k_1 = slope of the refrigerant saturation P-T curve at a given operating point
k_2 = spring Hooke's constant
$\dot{m}$ = mass flow rate
$\dot{m}_{ref}$ = refrigerant mass flow rate
P_b = pressure of the thermostatic element
P_{close} = closing pressure
P_{down} = downstream pressure
P_e = evaporator pressure
P_{open} = opening pressure
P_{sat} = saturated pressure
P_{static} = original static pressure setting
P_{up} = upstream pressure
$Cap_{reserve}$ = valve reserve capacity rate
T_{evap} = evaporator temperature
T_{sat} = saturated temperature
T_{sh} = superheat
$T_{sh,max,opening}$ = maximum opening superheat
$T_{sh,opening}$ = opening superheat
$T_{sh,operating}$ = operating superheat
$T_{sh,rating}$ = superheat at a rating condition
$T_{sh,rating,opening}$ = opening superheat at a rating condition
$T_{sh,static}$ = static superheat
T_{sub} = upstream refrigerant subcooling
x_{static} = static spring setting
ρ = fluid density
θ = valve disc angle

REFERENCES

ARI. 2001. *ARI Standard 750, Thermostatic Refrigerant Expansion Valves*. Arlington, VA: Air-Conditioning and Refrigeration Institute.

ASHRAE. 1998a. *ANSI/ASHRAE Standard 17, Method of Testing Capacity of Thermostatic Refrigerant Expansion Valves*. Atlanta, GA: American Society of Heating, Refrigerating and Air-Conditioning Engineers, Inc.

ASHRAE. 1998b. *ASHRAE Handbook—Refrigeration* (SI). Atlanta, GA: American Society of Heating, Refrigerating and Air-Conditioning Engineers, Inc.

Benjamin, M.W., and J.G. Miller. 1941. The flow of saturated water throttling orifice. *Transactions of the ASME* 63(5):419–26.

Browne, W.M., and Bansal, P.K. 1998. Challenges in modeling vapor-compression liquid chillers. *ASHRAE Transactions* 104(1):474–86.

Bullard, C.W. 2007. Designing systems to use simpler expansion devices, *Proceedings of the 22nd International Congress of Refrigeration, International Institute of Refrigeration, Beijing, China*, Paper # ICR07-E1-1330.

Chisholm, D. 1967. Flow of compressible two-phase mixtures through throttling devices. *Chemical and Process Engineering* 48(12):73–78.

Harms, T.M. 2002. Charge inventory system modeling and validation for unitary air conditioners. PhD thesis, School of Mechanical Engineering, Purdue University, West Lafayette, IN.

Kim, Y.C., D.L. O'Neal, W.V. Payne, and M. Farzad. 2002. Refrigerant flow through flexible short-tube orifices. *HVAC&R Research* 8(2):179–90.

Krakow, K.I., and S. Lin. 1988. Refrigerant flow through orifices. *ASHRAE Transactions* 94(1):484–506.

Li, H., and J.E. Braun. 2004. A methodology for diagnosing multiple-simultaneous faults in rooftop air conditioners. Tenth International Refrigeration and Air Conditioning Conference at Purdue, July 12–15.

Rice, C.K., and W.L. Jackson.1994. *The Mark V ORNL Heat Pump Design Model for Chlorine-Free, Pure and Near-Azeotropic Refrigerant Alternatives* (Documentation package, v0.95). Oak Ridge, TN: Oak Ridge National Laboratory